Review of Scientific Instruments

Diagnostics for studies of novel laser ion acceleration mechanisms

Cite as: Rev. Sci. Instrum. **85**, 113302 (2014); https://doi.org/10.1063/1.4900626
Submitted: 08 August 2014 . Accepted: 17 October 2014 . Published Online: 05 November 2014

Lovisa Senje, Mark Yeung, Bastian Aurand, Stephan Kuschel, Christian Rödel, Florian Wagner, Kun Li, Brendan Dromey, Vincent Bagnoud, Paul Neumayer, Markus Roth, Claes-Göran Wahlström, Matthew Zepf, Thomas Kuehl, and Daniel Jung

AIP Publishing

Diagnostics for studies of novel laser ion acceleration mechanisms

Lovisa Senje,[1] Mark Yeung,[2] Bastian Aurand,[1] Stephan Kuschel,[2] Christian Rödel,[2] Florian Wagner,[3] Kun Li,[4] Brendan Dromey,[5] Vincent Bagnoud,[2,6] Paul Neumayer,[4] Markus Roth,[3] Claes-Göran Wahlström,[1] Matthew Zepf,[2,5] Thomas Kuehl,[4,6,7] and Daniel Jung[5]
[1]*Department of Physics, Lund University, P. O. Box 118, S-221 00 Lund, Sweden*
[2]*Helmholtz-Institut Jena, D-07743 Jena, Germany*
[3]*Technische Universität Darmstadt, D-64289 Darmstadt, Germany*
[4]*ExtreMe Matter Institut, D-64291 Darmstadt, Germany*
[5]*Department of Physics and Astronomy, Queen's University, Belfast BT7 1NN, United Kingdom*
[6]*GSI Helmholtzzentrum für Schwerionenforschung GmbH, D-64291 Darmstadt, Germany*
[7]*Universität Mainz, D-55099 Mainz, Germany*

(Received 8 August 2014; accepted 17 October 2014; published online 5 November 2014)

Diagnostic for investigating and distinguishing different laser ion acceleration mechanisms has been developed and successfully tested. An ion separation wide angle spectrometer can simultaneously investigate three important aspects of the laser plasma interaction: (1) acquire angularly resolved energy spectra for two ion species, (2) obtain ion energy spectra for multiple species, separated according to their charge to mass ratio, along selected axes, and (3) collect laser radiation reflected from and transmitted through the target and propagating in the same direction as the ion beam. Thus, the presented diagnostic constitutes a highly adaptable tool for accurately studying novel acceleration mechanisms in terms of their angular energy distribution, conversion efficiency, and plasma density evolution. [http://dx.doi.org/10.1063/1.4900626]

I. INTRODUCTION

The field of laser-based ion acceleration has made significant advances over the last years.[1] Protons and other ions can be accelerated to high energies (MeVs) on a micrometre scale (compared to metre scale in conventional radio frequency accelerators) in plasmas from different materials placed in the focus of a high intensity laser beam. One of the currently most studied mechanisms for laser ion acceleration is target normal sheath acceleration[2,3] (TNSA), where ions are accelerated to tens of MeV from foils with thicknesses on the micrometre scale. Other acceleration schemes have been proposed and investigated through particle in cell (PIC) simulations, such as Radiation Pressure Acceleration[4,5] (RPA) and the Break-Out Afterburner[6,7] (BOA), and ions could here reach significantly higher energies of hundreds of MeV. These mechanisms demand very high laser intensities and/or high temporal laser contrast and only recent improvements in available laser systems[8,9] have allowed to experimentally study them.[10–15] With these new mechanisms characteristics significantly different from those of TNSA appear, such as monoenergetic ion spectra for RPA[16] and off-axis angular effects in ion beam profiles for BOA.[17] Further appearing, for both RPA and BOA, is the possibility to more efficiently accelerate heavier ions and changes in the characteristics of the laser radiation that is transmitted or reflected from the target.[18,19]

However, to distinguish and quantify the differences between the different acceleration mechanisms requires dedicated diagnostics. This is challenging to achieve, especially considering the often large angle of divergence of beams of laser accelerated ions of up to 40°.[20] Traditionally, stacks of radiochromatic film (RCF),[21] which changes color when absorbing radiation, and Thomson parabolas[22] have been used as main diagnostics. The disadvantages of these are that the RCF stacks provide limited energy resolution, have no means of separating different ion species, and make it difficult to simultaneously measure the laser spectrum, and that the Thomson parabola lacks angular resolution. Previously, the ion wide angle spectrometer[23] (iWASP) has been introduced as an initial cover of this need. Here, angularly resolved proton spectra can be obtained and a second ion species can also be recorded, although without charge information, making separation of multiple heavier ion species nearly impossible.

In this article, we present novel diagnostics that allow to experimentally distinguish different laser ion acceleration mechanisms: proton and ion spectra (for multiple species) along selected axes can be recorded simultaneously with the wide angle spectrum and the reflected and transmitted laser spectra. This diagnostic thereby makes it possible to study all the characteristics discussed above, simultaneously.

II. DESIGN

The design of the diagnostics has been made with focus on features particularly important to investigate in order to distinguish different laser ion acceleration mechanisms: (I) Angularly resolved energy spectra for protons and one more ion species, (II) Spectrum for each ion species present along selected axes, and (III) Characteristics of laser radiation transmitted and reflected from the target.

A. Ion wide angle spectrometer

Charged particles, such as ions, passing through a magnetic dipole field obtain a curved trajectory characterised by

the Larmor radius, which can be derived from the magnetic part of the Lorentz equation,

$$\vec{F} = q(\vec{v} \times \vec{B}), \tag{1}$$

where $\vec{F}$ is the force exerted on a particle with charge, q, and velocity, $\vec{v}$, by the magnetic field, $\vec{B}$. Such magnetic field can, for example, be set up between two parallel permanent magnets, acting as a basic ion spectrometer. As mentioned before, beams of laser accelerated ions can be highly divergent and a pinhole or a slit at the entrance of the ion spectrometer is thus necessary in order to separate the different ion energies with sufficient resolution. With such a spectrometer it is however not possible to resolve angular features in the divergent beams of laser accelerated ions and thereby not meeting requirement (I). In an iWASP, this is resolved by using a wide entrance slit and an angle between the magnets, see Fig. 1, and thus allowing a larger part of a divergent beam to reach the detector. A major difference between the iWASP and a standard ion spectrometer is thereby the much larger solid angle covered.[23,24]

The magnetic field in an iWASP is not exactly equal for all angles α, see Fig. 1(b), and, in addition, particles moving in different directions travel different distances both inside and outside the iWASP before reaching the detector. For small particle deflections inside the magnetic field, the vertical displacement of a non-relativistic ion with mass m, on a detector located a distance d_B after the end of the magnetic field is given by

$$D_B(\alpha) = \frac{qB_\perp(\alpha)L_B(\alpha)}{mv_\alpha}\left(\frac{L_B(\alpha)}{2} + d_B(\alpha)\right), \tag{2}$$

where D_B is the displacement, $B_\perp$ is the component of the magnetic field in the horizontal plane directed perpendicular to the ion trajectory, v_α is the velocity component directed at an angle α from the z-direction, and L_B is the length of the magnetic field.

In the detector plane of the iWASP, the ion energies are thus given by their vertical position and their angular properties along the horizontal axis. Along the axis of the entrance slit the iWASP thereby gives an angularly resolved ion energy spectrum (requirement (I) above).

B. Ion separation extension (ISE)

The magnetic fields of neither a basic magnetic ion spectrometer nor an iWASP, can separate multiple different ion species. This can be remedied by letting the ions pass through an electric field $\vec{E}$, which exerts a force

$$\vec{F} = q\vec{E} \tag{3}$$

on a particle with charge q.

Traditionally, in a Thomson parabola, where a magnetic ion spectrometer is combined with high voltage electrodes, only one detector plane is used and electrodes are placed inside or directly after the magnet. This is not possible with an iWASP since the traces of different ion species would be overlapping.

To fulfil requirement (II) above and separate multiple ion species, and at the same time maintaining requirement (I), a thin, vertical slit is made in the detector plane of the iWASP,

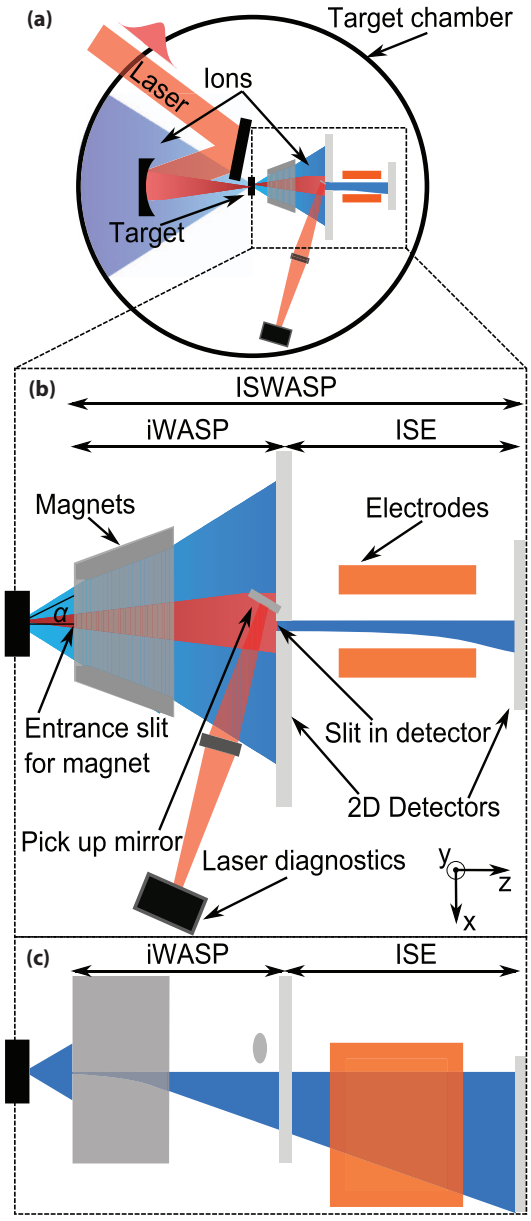

FIG. 1. (a) A schematic topview of a possible experiment chamber setup where the incoming laser beam is focused onto the target at normal incidence by an off-axis parabolic mirror. (b) Topview of close-up of laser and ion diagnostics (ISWASP). The ions first pass through an ion wide angle spectrometer (iWASP), providing energy dispersion. Some of the ions propagate through a slit in the first detector plane, into an ion separation extension (ISE) unit. Here, the ions pass through an electric field, providing separation according to the ions' charge to mass ratio, onto a second detector. The 2-dimensional detectors could, for example, consist of image plates and/or nuclear track detectors (CR39). Laser radiation transmitted through the target is diffracted in the entrance slit of the iWASP and thereafter picked up by a mirror located outside the ion beam and guided onto laser diagnostics. (c) Sideview of (b). In this dimension, the divergence of the ion beam is reduced due to the entrance slit of the iWASP. The laser light is here omitted for clarity but the pick-up mirror is shown above the ion beam.

positioned in the target normal direction (0°) in Fig. 1. It could however be placed along any arbitrary axis directed at an angle α from the target normal, inside the acceptance angle of the iWASP. The slit is perpendicular to the entrance slit of the iWASP and they are thereby together forming a

rectangular "pinhole." Behind this "pinhole" two high voltage copper electrodes are placed. This extension separates the different ion species in a direction perpendicular to the magnetic displacement when a high voltage is applied to the electrodes. The deviation from the original axis for a non-relativistic ion caused by the $\vec{E}$-field is given by

$$D_E = \frac{qE_x L_E}{mv_\alpha^2}\left(\frac{L_E}{2} + d_E\right), \tag{4}$$

where D_E denotes the displacement, m is the mass of the ion, L_E is the length of the electric field, and d_E is the distance to the detector plane from the end of the electric field.

After the electrodes an additional detector is located to record the ion traces. With this extension we add the capability of ion separation and of recording spectra for several ion types to the iWASP, together forming the ion separation wide angle spectrometer (ISWASP). It is further also possible to use several extensions in different directions in a multi-ISWASP configuration.

The resolution of the ISE is limited by properties of the electric field, such as strength and length, and the size of the rectangular "pin hole." The height of the first slit determines the energy resolution whereas the width of the second slit affects the width of the traces and thereby how well the ion traces from different species are separated. The vertical slit should be chosen as wide as possible, while still allowing the different ion traces to be separated, in order to maximize the signal to noise level on the detector.

The distances between the different components of the diagnostics can be varied, as well as the voltages applied to the electrodes, making it possible to tune the diagnostic for different circumstances. It is therefore a versatile instrument suitable to use with a wide range of particle energies.

C. Characterization of transmitted and reflected laser radiation

In the presented design, we utilize the fact that a significant amount of laser light can be collected through the entrance slit of the ISWASP to cover requirement (III). This allows simultaneous recording of the laser light transmitted and reflected from the target along with the ion spectra. A pick-up mirror is placed in front of the first detector plane. We exploit that any part of the laser pulse transmitted through the target foil will diffract in the slit of the ISWASP, making it possible to place a pick-up mirror in such a way that it does not affect or clip the ion beam or the zero-order (neutral particles that are unaffected by the electric and magnetic field), see Fig. 1(c). The pick-up mirror reflects the light into an optical diagnostic instrument. The incident laser light which is reflected on the target is recollimated by the focusing optics and a fraction is picked up by a leakage from one of the mirrors in the beam path.

In a simple version, integrating diagnostic can be used for both the transmitted and reflected laser light. In order to fully resolve the dynamics, an auto-correlator or a Frequency-Resolved Optical Gating[25] (FROG) could be used, providing further information about the temporal evolution of the transient plasma dynamics.

III. IMPLEMENTATION

The proposed design of the ISWASP has been tested at the PHELIX laser[26] at GSI Helmholtzzentrum für Schwerionenforschung GmbH, Germany. Protons and carbon ions were accelerated from nanometre thin parylene foils[27,28] by a 80 J, 500 fs laser pulse with a central wavelength of 1053 nm, which could be made circularly polarized by using a quarter-wave plate. The laser pulse was interacting with the target at normal incidence.

Ion and proton spectra were recorded simultaneously with the ISWASP. The iWASP-section used consists of two 10 cm long permanent magnets mounted in an iron yoke with a half angle of 15° and a horizontal entrance slit positioned on the front. The magnetic field between the magnets is approximately 0.4 T. The detector plane of the iWASP was positioned 500 mm from the source. In the implementation of this design, the particle detectors of the iWASP were image plates[29] covered with a layer of 1 mm thick CR39[30] in the region where protons above 10 MeV are expected. Protons with such energies will pass through the layer onto the image plate, whereas the heavier ions will be stopped in the CR39. The damage in the CR39 caused by protons at these energies is negligible and only visible after long etching times. The angularly resolved proton spectrum and the spectrum of the carbon ions were detected on the image plate and CR39, respectively. The entrance slit of the ISE measured 120 μm and was positioned in the target normal direction, $\alpha = 0°$. The electrodes of the ISE were 100 mm long, separated by 16 mm, and had an applied voltage of 7 kV. The detector of the ISE was placed 800 mm from the source and consists of an image plate. Ion traces in the ISE were obtained for protons, C^{6+} and C^{5+}, see Fig. 2. The optical axis is not visible in the figure but corresponds to the point where both $\vec{E}$-field and $\vec{B}$-field deflections are zero. The diagnostics can easily be adjusted for different target materials, giving other ion species, by changing the voltage on the electrodes and/or the distance from the electrodes to the detector plane.

The traces on the image plate can be analysed starting from Eqs. (2) and (4) and the spectra for each ion species can thus be obtained. Spectra corresponding to the ion traces in Fig. 2 are found in Fig. 3. In the analysed spectra, a maximum energy of ~28 MeV was determined for protons and

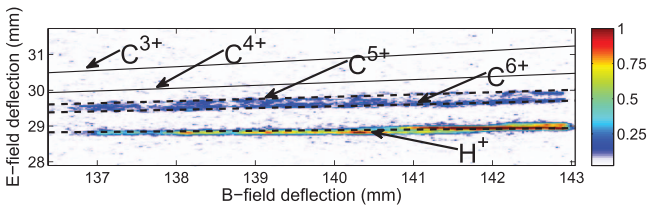

FIG. 2. Image plate with experimentally obtained ion traces from the ion separation extension (ISE) in combination with the ion wide angle spectrometer (iWASP). The dashed lines indicate simulated traces of H^+, C^{6+}, and C^{5+}, whereas the thin, solid lines indicate the simulated traces of C^{4+} and C^{3+}. The latter two traces and subsequently also carbon ions in lower charge states, were below the detection threshold for the experimental conditions under which the ISWASP was tested, as most carbon ions were then fully ionized. The color scale gives the photo stimulated luminescence of the image plate where one corresponds to the strongest signal.

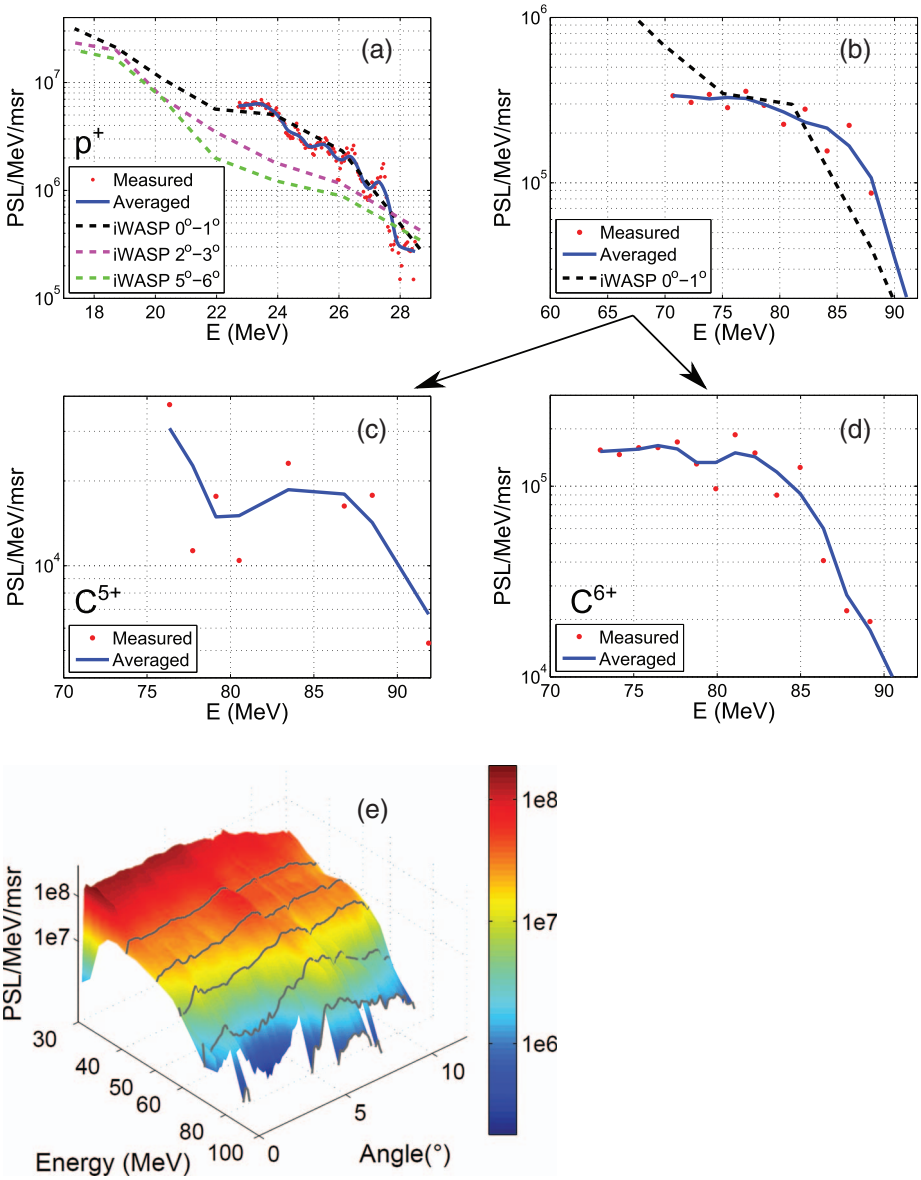

FIG. 3. Ion spectra obtained with an ISWASP, analysed from raw traces shown in Fig. 2. From the ISE-unit, the red dots indicate actual data points whereas the solid blue line is a moving average over several data points and are recorded from the ion separation extension. The dashed lines are spectra recorded with only the iWASP. On the vertical axes PSL stands for the photo stimulated luminescence of the image plates. For conversion of PSL to absolute particle numbers, an equipment specific calibration is required. (a) Proton spectra, the different angular intervals are defined so that 0° is directed in the target normal direction. (b) The carbon ion traces recorded with iWASP and CR39 as detector and the ISE using an image plate, in both cases assuming that only C^{6+} is present. Then in (c) (C^{5+}) and (d) (C^{6+}) the different species have been separated. (e) Carbon wide angle spectrum from iWASP, again assuming that only C^{6+} is present.

~90 MeV for both detected carbon charge states. It can also be seen in Fig. 3 that, as expected, the proton spectra from the iWASP converges into the one from the ISE as the angle moves towards 0° where the extension was placed. In the detector plane of the iWASP, carbon ions are detected with a CR39. The analysis of this has been done assuming that all carbon atoms were fully ionised to C^{6+}. In order to be able to compare with the ISE, the carbon traces in Fig. 2 were first analysed as if they both were C^{6+}. These spectra are shown together in Fig. 3(b). In Figs. 3(c) and 3(d), spectra can be seen from the ISE, where the two different charge states of carbon ions have been separated. From these spectra, the ratio between the number of C^{5+} and C^{6+} can also be deduced (in spectra from Fig. 3 this ratio is ~13%) and thereby giving an error estimate of the spectra in Figs. 3(b) and 3(e).

If a higher voltage is applied to the electrodes in the ISE, the separation between the different ion traces in Fig. 2 would become larger and thereby making the analysis easier for cases where there are many different species present.

The laser spectrum was recorded with optical spectrometers, both in the transmitted and the reflected direction, see Fig. 4 where the second order harmonic is shown. Red and blue-shifts can be compared for different shots for both the transmitted and reflected light and from this information about the plasma expansion from the laser-target interaction can be deduced. Shot to shot variations in the intensity ratio between the two light components can also be analysed.

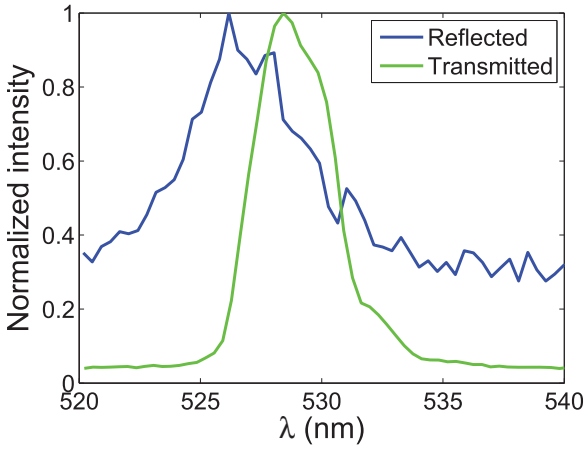

FIG. 4. The second order harmonic of the laser spectrum reflected from (blue) and transmitted through (green) the target. The former recollimated by the focusing optics and recorded through a leakage of a mirror in the laser beam path and the latter picked up from diffraction from the entrance slit of the ISWASP.

IV. CONCLUSIONS

A novel diagnostics, the ISWASP, is presented with the major advantage that multiple parameters can be investigated simultaneously, minimizing the impact of shot-to-shot fluctuations. This is especially important when taking into account the current repetition rate at many high power laser facilities (commonly as low as ∼1/h), which makes it challenging to acquire large data sets. The diagnostic presented here gives highly useful additional information compared to only using a RCF stack, a Thomson parabola, or an iWASP, in particular for distinguishing between different laser ion acceleration mechanisms. In this first experiment, the ISE was used only along the optical axis, but it could be positioned along any axis in the detection plane of the iWASP and multiple extensions could also be used simultaneously allowing ion separation along different axes.

ACKNOWLEDGMENTS

The research leading to these results has received funding from LASERLAB-EUROPE (Grant Agreement No. 284464, EC's Seventh Framework Programme) and the Swedish Research Council. L. Senje acknowledges financial support from SILMI, European Science Foundation (ESF).

[1]A. Macchi, M. Borghesi, and M. Passoni, Rev. Mod. Phys. **85**, 751–793 (2013).
[2]S. P. Hatchett, C. G. Brown, T. E. Cowan, E. A. Henry, J. S. Johnson, M. H. Key, J. A. Koch, A. B. Langdon, B. F. Lasinski, R. W. Lee, A. J. Mackinnon, D. M. Pennington, M. D. Perry, T. W. Phillips, M. Roth, T. C. Sangster, M. S. Singh, R. A. Snavely, M. A. Stoyer, S. C. Wilks, and K. Yasuike, Phys. Plasmas **7**, 2076 (2000).
[3]S. C. Wilks, A. B. Langdon, T. E. Cowan, M. Roth, M. Singh, S. Hatchett, M. H. Key, D. Pennington, A. MacKinnon, and R. A. Snavely, Phys. Plasmas **8**, 542 (2001).
[4]T. Esirkepov, M. Borghesi, S. V. Bulanov, G. Mourou, and T. Tajima, Phys. Rev. Lett. **92**, 175003 (2004).
[5]A. Macchi, F. Cattani, T. V. Liseykina, and F. Cornolti, Phys. Rev. Lett. **94**, 165003 (2005).
[6]L. Yin, B. J. Albright, B. M. Hegelich, K. J. Bowers, K. A. Flippo, T. J. T. Kwan, and J. C. Fernandez, Phys. Plasmas **14**, 056706 (2007).
[7]B. J. Albright, L. Yin, K. J. Bowers, B. M. Hegelich, K. A. Flippo, T. J. T. Kwan, and J. C. Fernandez, Phys. Plasmas **14**, 094502 (2007).
[8]R. C. Shah, R. P. Johnson, T. Shimada, K. A. Flippo, J. C. Fernandez, and B. M. Hegelich, Opt. Lett. **34**, 2273 (2009).
[9]A. Jullien, O. Albert, F. Burgy, G. Hamoniaux, J.-P. Rousseau, J.-P. Chambaret, F. Aug-Rochereau, G. Chriaux, J. Etchepare, N. Minkovski *et al.*, Opt. Lett. **30**, 920 (2005).
[10]A. Henig, S. Steinke, M. Schnürer, T. Sokollik, R. Hörlein, D. Kiefer, D. Jung, J. Schreiber, B. M. Hegelich, X. Q. Yan, J. Meyer-ter Vehn, T. Tajima, P. V. Nickles, W. Sandner, and D. Habs, Phys. Rev. Lett. **103**, 245003 (2009).
[11]D. Jung, L. Yin, D. C. Gautier, H.-C. Wu, S. Letzring, B. Dromey, R. Shah, S. Palaniyappan, T. Shimada, R. P. Johnson, J. Schreiber, D. Habs, J. C. Fernández, B. M. Hegelich, and B. J. Albright, Phys. Plasmas **20**, 083103 (2013).
[12]B. Aurand, S. Kuschel, O. Jäckel, C. Rödel, H. Y. Zhao, S. Herzer, A. E. Paz, J. Bierbach, J. Polz, B. Elkin *et al.*, New J. Physics **15**, 033031 (2013).
[13]B. Aurand, S. Kuschel, O. Jäckel, C. Rödel, H. Zhao, S. Herzer, A. Paz, J. Bierbach, J. Polz, B. Elkin *et al.*, Nucl. Instrum. Methods Phys. Res. A **740**, 83–86 (2014).
[14]C. A. J. Palmer, N. P. Dover, I. Pogorelsky, M. Babzien, G. I. Dudnikova, M. Ispiriyan, M. N. Polyanskiy, J. Schreiber, P. Shkolnikov, V. Yakimenko, and Z. Najmudin, Phys. Rev. Lett. **106**, 014801 (2011).
[15]S. Kar, K. F. Kakolee, B. Qiao, A. Macchi, M. Cerchez, D. Doria, M. Geissler, P. McKenna, D. Neely, J. Osterholz, R. Prasad, K. Quinn, B. Ramakrishna, G. Sarri, O. Willi, X. Y. Yuan, M. Zepf, and M. Borghesi, Phys. Rev. Lett. **109**, 185006 (2012).
[16]A. P. L. Robinson, M. Zepf, R. G. Kar, S. Evans, and C. Bellei, New J. Phys. **10**, 013021 (2008).
[17]L. Yin, B. J. Albright, K. J. Bowers, D. Jung, J. C. Fernández, and B. M. Hegelich, Phys. Rev. Lett. **107**, 045003 (2011).
[18]S. Palaniyappan, B. M. Hegelich, H.-C. Wu, D. Jung, D. C. Gautier, L. Yin, B. J. Albright, R. P. Johnson, T. Shimada, S. Letzring, D. T. Offermann, J. Ren, C. Huang, R. Hörlein, B. Dromey, J. C. Fernandez, and R. C. Shah, Nat. Phys. **8**, 763 (2012).
[19]A. Macchi, S. Veghini, T. V. Liseykina, and F. Pegoraro, New J. Phys. **12**, 045013 (2010).
[20]A. Maksimchuk, S. Gu, K. Flippo, and D. Umstadter, Phys. Rev. Lett. **84**, 4108–4111 (2000).
[21]F. Nürnberg, M. Schollmeier, E. Brambrink, A. Blazevic, D. C. Carroll, K. Flippo, D. C. Gautier, M. Geissel, K. Harres, B. M. Hegelich, O. Lundh, K. Markey, P. McKenna, D. Neely, J. Schreiber, and M. Roth, Rev. Sci. Instrum. **80**, 033301 (2009).
[22]J. J. Thomson, Philos. Mag. Ser. 6 **22**, 469 (1911).
[23]D. Jung, R. Hörlein, D. C. Gautier, S. Letzring, D. Kiefer, K. Allinger, B. J. Albright, R. Shah, S. Palaniyappan, L. Yin, J. C. Fernandez, D. Habs, and B. M. Hegelich, Rev. Sci. Instrum. **82**, 043301 (2011).
[24]D. Gwynne, S. Kar, D. Doria, H. Ahmed, M. Cerchez, J. Fernandez, R. J. Gray, J. S. Green, F. Hanton, D. A. MacLellan *et al.*, Rev. Sci. Instrum. **85**, 033304 (2014).
[25]D. Kane and R. Trebino, IEEE J. Quantum Electron. **29**, 571–579 (1993).
[26]V. Bagnoud, B. Aurand, A. Blazevic, S. Borneis, C. Bruske, B. Ecker, U. Eisenbarth, J. Fils, A. Frank, E. Gaul *et al.*, Appl. Phys. B **100**, 137–150 (2010).
[27]B. Aurand, B. Elkin, L.-O. Heim, B. Lommel, B. Kindler, M. Tomut, C. Rödel, S. Kuschel, O. Jäckel, J. Barz *et al.*, J. Polym. Sci. Part B: Polym. Phys. **51**, 1355–1360 (2013).
[28]B. Aurand, B. Elkin, L.-O. Heim, B. Lommel, B. Kindler, M. Tomut, C. Rödel, S. Kuschel, O. Jäckel, and T. Kuehl, J. Radioanal. Nucl. Chem. **299**, 965 (2014).
[29]I. J. Paterson, R. J. Clarke, N. C. Woolsey, and G. Gregori, Meas. Sci. Technol. **19**, 095301 (2008).
[30]R. L. Fleischer, P. B. Price, and R. M. Walker, J. Appl. Phys. **36**, 3645 (1965).